

Preparation and characterization of functional material based on hybrid polymer composites

La Agusu¹, Amiruddin², Chen Chen Taswito², Herdianto² and Muh. Zamrun¹

¹Department of Physics, University of Halu Oleo, Kendari, Indonesia

²Department of Chemistry, University of Halu Oleo, Kendari, Indonesia

E-mail address: la_agusu@yahoo.com

Abstract. The microstructures and properties of hybrid polymer composites based on polyaniline (PANi)/ γ -Fe₂O₃ nanoparticles/TiO₂/carbon have been investigated for multi-functional applications such as heavy metal removal and initial study for radar absorbing material application. γ -Fe₂O₃ nanoparticles with spherical shape were synthesized by a co-precipitation method from iron sand. By activating the polyethylene glycol (PEG-400) coated carbon of coconut shell, the homogenous shape and size of carbon was achieved. Then, γ -Fe₂O₃, TiO₂, and carbon were mixed with PANi by an in situ polymerization method at low temperature 0-5 °C. Characterization process involved XRD, SEM, FTIR, VSM, and DC conductivity measurements. For radar absorber application, the functionalized polymer composites showed good electrical conductivity 0.45 S/cm to absorb the incoming electromagnetic energy. An efficient and effective reduction of Pb²⁺ ion from the water has been achieved by using this material.

1. Introduction

Development of the functional materials based on conducting polymer is an interesting topic of research due to its potential application such as radar absorbing materials (RAM) [1], energy storage [2], sensor [3], water treatment [4], etc. Conducting polymer based materials has many advantages in its high conductivity and stability, cheap, lightweight, easy to use, etc. In RAM applications, conducting polymer loaded by different kind materials such as magnetic and dielectrics can increase its ability to absorb the energy of radar waves that can minimize the reflected signal in noise level. In the presence of conducting fillers, an electrically conducting polymer matrix has the added advantage of being able to electrically connect the filler units that do not touch one another, thereby enhancing connectivity. While the magnetic materials tend to absorb radar waves at lower frequencies, the dielectric materials cover at much higher frequencies. By combining them, one may tune the absorption frequency as well as its absorption bandwidth through tuning its permittivity and permeability constant.

In water treatment application, the functional variation of organic materials that were combined with advantages of a thermally stable and robust inorganic substrate, will result in strong binding affinities toward selected metal ions and relatively high metal ion adsorption capacities. Functionalized hybrid polymeric materials as adsorbent are regarded as one of the most effective techniques because metal ions can be chemically bonded by the organic-inorganic polymer hybrids. Incorporating magnetic nanoparticles make easy in application because it can easily separated by using the external magnetic field.



In this report we synthesized the functional materials based on mixing of polyaniline (PANI) with $\gamma\text{-Fe}_2\text{O}_3$ nanoparticles, carbon of coconut shell, and TiO_2 to form PANi/ $\gamma\text{-Fe}_2\text{O}_3$ /TiO₂/carbon. $\gamma\text{-Fe}_2\text{O}_3$ nanoparticles were synthesized by a co-precipitation method for iron sand. Its performances as RAM and Pb metal ion absorption were evaluated.

2. Materials and methods

2.1. Synthesis of $\gamma\text{-Fe}_2\text{O}_3$ nanoparticles

After separation of iron powders from iron sands and cleaning process from any impurities with distilled water and acetone, respectively, then iron powders were dried in an oven at 60°C for 24 hours. A 20 gr of iron powders were dissolved in 12 M 50 ml HCl at a constant temperature of ~60 °C and under stirring condition. Then solution was filtered and transferred to the three neck round bottom flask. The precipitating solution, 6M NH_4OH , was prepared and added dropwise to the previous solution. The temperature was kept at ~60°C. Just after mixing solution, color changed from light brown to brown indicating the forming of $\gamma\text{-Fe}_2\text{O}_3$ nanoparticles, which was allowed to crystalline completely for another 6 min under rapid stirring. The final reaction pH was measured. The precipitated solution were centrifugated, washed, and dried at temperature 60°C for 24 hour. Finally, $\gamma\text{-Fe}_2\text{O}_3$ powder nanoparticles were collected and characterized.

2.2. Preparation of carbon from coconut shell

The coconut shell was cleaned and dried for 2 days. Then it was crushed reduce the size. A 250g of the smaller pieces was carbonized at 400°C for 30 minutes. It was then washed several times with distilled water until a pH range between 6 and 7 was obtained. The sample was then dried in an oven at 105 °C for 24 hours. The dried sample was sieved to pass 63 micron mesh and subsequently mixed with 10% wt of polyethylene glycol (PEG-400). The PEG coated carbon was then transferred to electric furnace at 350 °C for 30 minutes. After cooling down the carbon with more homogenous shapes and sizes were achieved.

2.3. Synthesis of PANi/ $\gamma\text{-Fe}_2\text{O}_3$ /TiO₂/carbon

The functional material PANi/ $\gamma\text{-Fe}_2\text{O}_3$ /TiO₂/Carbon was synthesized by in situ polymerization method at low temperature 0-5 °C. PANi was mixed with $\gamma\text{-Fe}_2\text{O}_3$ nanoparticles, anatase TiO₂, and carbon with weight ratio of aniline/ $\gamma\text{-Fe}_2\text{O}_3$ /TiO₂/carbon is 1:1:1:1. Anatase TiO₂ was prepared separately by sieving TiO₂ powder to pass #250 mesh and subsequently calcined in electric furnace at 800 °C for 2 hours. Aniline solution 1 M 25 mL was dissolved in HCl solution 1 M 25 mL under continuous stirring for 2 hours at temperature of 0-5 °C. Then $\gamma\text{-Fe}_2\text{O}_3$ nanoparticles, anatase TiO₂, and carbon were added to aniline hydrochloride solution under continuous stirring for another one hour. After adding $(\text{NH}_4)_2\text{S}_2\text{O}_8$ solution 1 M 25 mL to previous solution colour change to green indicating the polymerization process. The final solution was stirred over night for another 12 hours, filtered, washed, and dried at 60 °C for 24 hours.

2.4. Characterization process

Characterization process involved x-ray diffraction (XRD) for crystalline size, scanning electron microscope (SEM) for surface morphology, magnetization curve with vibrating sample magnetometer (VSM), FTIR for active functional group identification, electrical conductivity measurement with two probe method, and chemical element determination using atomic absorption spectroscopy (AAS).

3. Results and discussion

Here, we adjusted pH from 6.5 to 12 by slowly dropping of NH_4OH solution. $\gamma\text{-Fe}_2\text{O}_3$ nanoparticles with high purity verified by XRD spectral were evidently obtained at pH 8 until 12. In this report we discuss the characteristic of as synthesized $\gamma\text{-Fe}_2\text{O}_3$ at pH 10 only. Other pH conditions will be discussed and published separately. The XRD pattern in Figure 1 shows sharp peaks, with major peaks

at (311) and (440), indicating good crystallinity of the obtained product. The XRD peaks match with $\gamma\text{-Fe}_2\text{O}_3$ peaks (JCPDS card no. 39-1364). Averaged crystal size of about 24.47 ± 4.18 nm was calculated by fitting the XRD peaks with Lorentzian profiles using the Xpovder software [5]. This were confirmed with a modarate resolution of SEM image shown in Figure 2. The particles are almost spherical with the particle size of several tens nanometer.

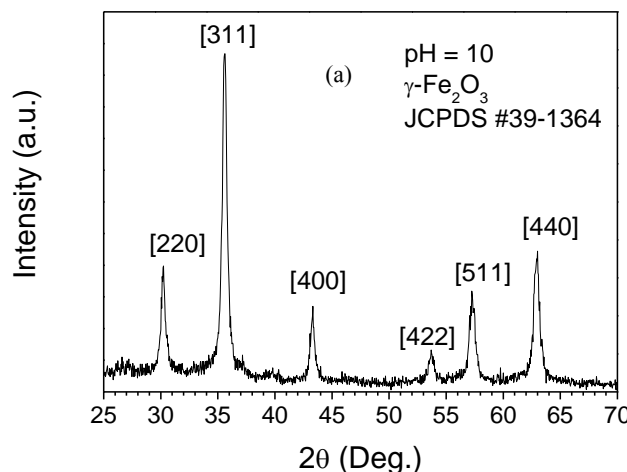


Figure 1. XRD pattern of as synthesized sample at pH 10. Some crystal planes of maghemite (JCPDS card no. 39-1364) are indicated on the peaks.

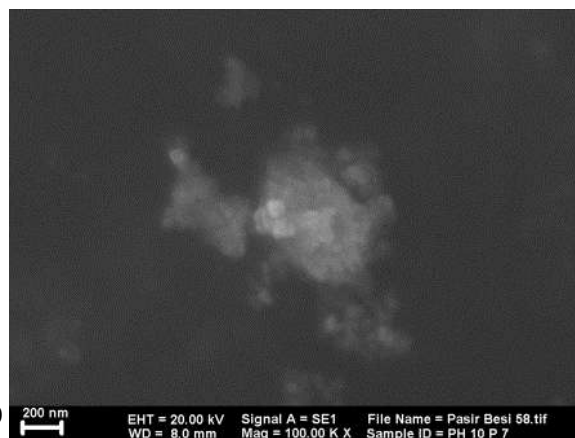


Figure 2. SEM image of as synthesized sample for pH 10. Particles tends to be spherical. with particle size several tens nanometer

The dependence of the external magnetic field on magnetization for $\gamma\text{-Fe}_2\text{O}_3$ was shown in Figure 3. The saturation magnetization reaches 59.3 emu/g. It was seen in Figure 3 that the hysteresis effect was observed with a relatively small coercivity field of 97.05 Gauss and a relatively high magnetic remanen of 8.48 emu/g. This was a typical property of soft magetic materials. Unfortunately, the superparamagnetic condition were not achieved yet. This may caused by the non-uniform particle size. The particles where the size is larger than nanometer exhibit a hysteresis effect on the magnetization curve, hindering the superparamagnetic property of the smaller ones to occur.

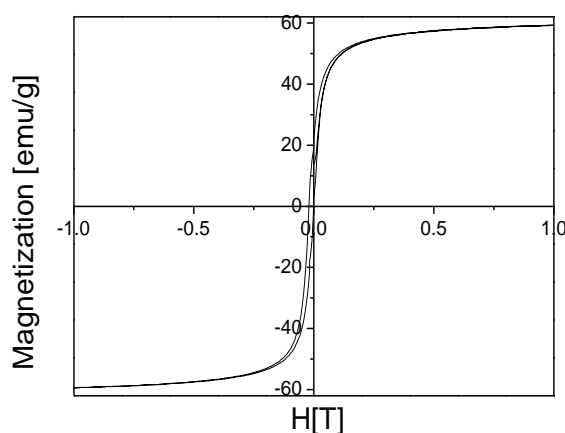


Figure 3. Magnetization cuve of $\gamma\text{-Fe}_2\text{O}_3$ synthesized at pH 10..

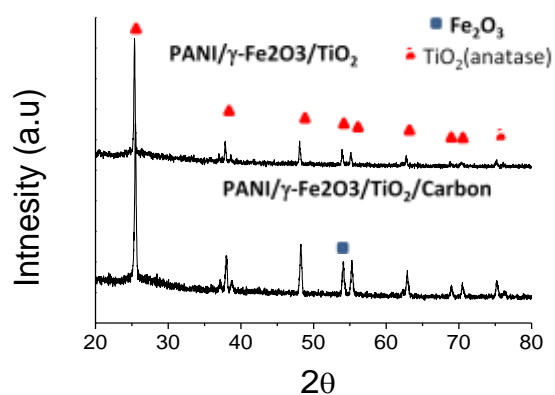


Figure 4. XRD peaks of hybrid conducting polymer: PANi/ $\gamma\text{-Fe}_2\text{O}_3$ /TiO₂ (upper part) and PANi/ $\gamma\text{-Fe}_2\text{O}_3$ /TiO₂/carbon (bottom)

Figure 4 shows XRD pattern of PANi/ γ -Fe₂O₃/TiO₂/carbon (upper part) compared to the spectrum of PANi/ γ -Fe₂O₃/TiO₂ (bottom). The anatase TiO₂ dominated the crystalline phase of TiO₂. XRD peaks of γ -Fe₂O₃ occurs overlap with diffraction peaks of TiO₂. For example peak found at $2\theta=53.11^\circ$ corresponds to crystalline of γ -Fe₂O₃.

Figure 5 shows SEM image of PANi/ γ -Fe₂O₃/TiO₂/carbon. It is seen that the particles are almost spherical shapes. The bright color corresponds to TiO₂ and the particles with dark colors for γ -Fe₂O₃ and carbon. Coating process with PEG-400 has successfully homogenized the size and shape of carbon of coconut shell after activation process. The FTIR spectral of functional material compared to pure Fe₂O₃ and PANi are shown in Figure 6. Functionalization of PANi/ γ -Fe₂O₃/TiO₂/carbon was shown clearly by shifting absorption spectra of Fe-O bond from 3404.2 cm⁻¹ to 3201 cm⁻¹ (O-H stretching) or shifting of absorption spectra of PANi from 3120.7 cm⁻¹ (C-H stretching) to 3201 cm⁻¹ (O-H stretching).

The functional material PANi/ γ -Fe₂O₃/TiO₂/carbon shows a high electrical conductivity $\sigma = 0.45$ S/cm. The electrical conductivity will contribute to imaginary part of the complex electrical permittivity of material simply in the form $\varepsilon = \varepsilon' - j\sigma/\omega$ where ε' and ω are real electrical permittivity and frequency. High value of electrical conductivity can increase the imaginary part of ε then will increase absorption capability of the material. Theoretically, one mechanism of RF energy absorption is an eddy current effect. RF field induce the electric current transferred through out material via its electrical conductivity converted to heat. The polyaniline, in this composite, may act as a conducting channel that connect γ -Fe₂O₃, TiO₂, and carbon. Furthermore, incorporating magnetic material into resistive material such as carbon could improve its absorption capability through the imaginary part of magnetic permeability $\mu = \mu' - i\mu''$. Radar waves induce a molecular oscillations from the alternating magnetic field of radar energy into heat. The value of ε and μ of the materials are frequency dependent, then by adjusting their characteristics a broadband absorber could be realized. Hybrid conducting polymer is a promising material for such interesting application.

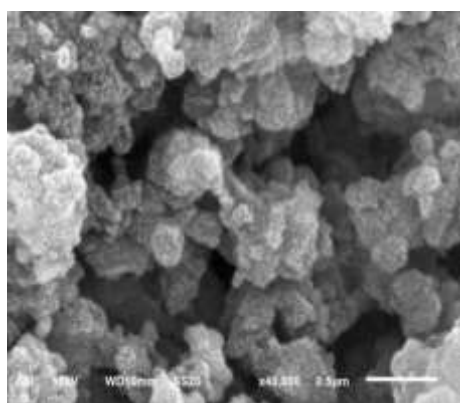


Figure 5 SEM functional material PANi/ γ -Fe₂O₃/TiO₂/carbon

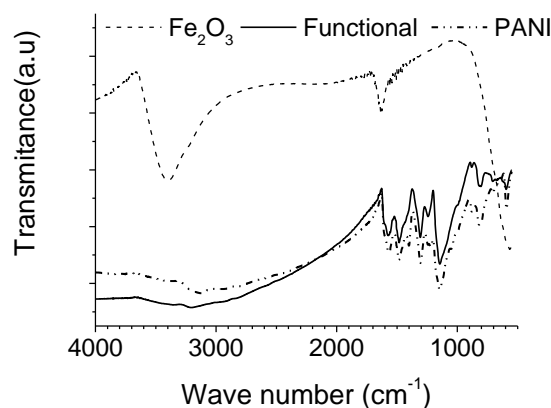


Figure 6 FTIR spectrum of Fe₂O₃, PANi/ γ -Fe₂O₃/TiO₂/carbon, and PANi

Another challenging application investigated here is using this functionalized material for absorbing heavy metal ion particularly Pb metal ions from the water. The initial concentration of Pb²⁺ ion is 94 ppm measured by AAS. After adding 54 ppm of functional material to Pb contaminated water, the solution left for 24 hours. Figure 7(a) shows absorption capability of PANi/ γ -Fe₂O₃/TiO₂/carbon to Pb²⁺ ions for different pH conditions. It is seen that the maximum absorption capability of about 92.4% is achieved at pH = 6. After then absorption drop to half at pH = 8 and

completely not effective at $\text{pH} > 9$. Figure 7(b) show absorption versus time contact between pollutant and absorbant for $\text{pH} = 6$. The interaction time of about 30 minutes can effectively remove Pb^{2+} ions from the water. It is shorter than if the stand alone nanoparticles $\gamma\text{-Fe}_2\text{O}_3$ or Fe_3O_4 used for water treatment that need several hours interaction time [6]. The advantage of using paramagnetic material like $\gamma\text{-Fe}_2\text{O}_3$ is easy to be separated from pollutant by using an external magnetic field.

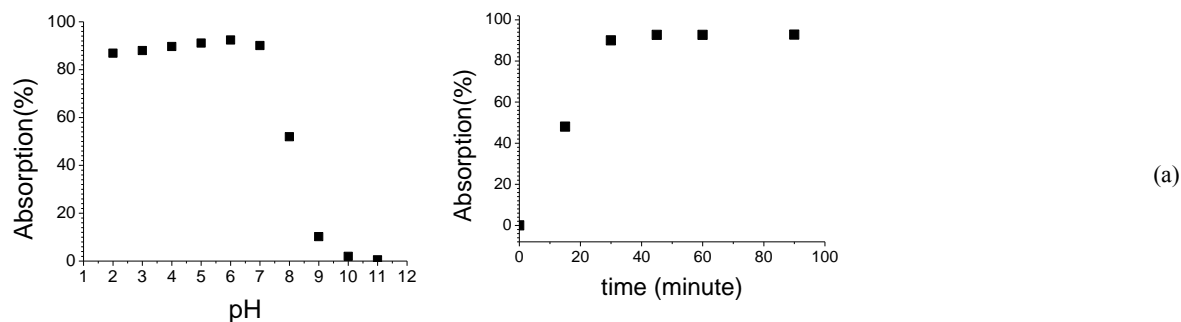


Figure 7. Adsorption capability of PANi/ $\gamma\text{-Fe}_2\text{O}_3$ /TiO₂/carbon to Pb^{2+} ions in the water. (a) absorption vs. pH for initial concentration of Pb^{2+} ions 94 ppm, and (b) absorption vs. interaction time at $\text{pH} = 6$.

4. Conclusion

In this report, $\gamma\text{-Fe}_2\text{O}_3$ nanoparticles has been synthesized with both high purity by a co-precipitation method from iron sand. The particle sizes is approximately 24.47 ± 4.18 nm and has rounded shape. The saturated magnetization is 59.3 emu/g. Another finding is that by using PEG-400 for coating carbon of coconut shell before activation process gives also spherical shape of carbon which is more difficult to achieve without coating. The conductivity of functional material PANi/ $\gamma\text{-Fe}_2\text{O}_3$ /TiO₂/carbon is high enough of around 0.45 S/cm and suitable for RAM applications. Fast and efficient removal of Pb^{2+} ions from water has been demonstrated using PANi/ $\gamma\text{-Fe}_2\text{O}_3$ /TiO₂/carbon. Another advantage of using this for removing water pollutant is easily taken out from the water by using a permanent magnet.

Acknowledgments

This research was partially supported by Research Grant of Fundamental Research from Ministry of Research and Higher Education, Republic of Indonesia, under grant agreement no. 063-3/PPK/UHO/IV/2014.

5. References

- [1] X. Zhao, Z. Zhang, L. Wang, K. Xi, Q. Cao, D. Wang, Y. Yang, and Y. Du, Scientific Reports **3**, 341 (2013).
- [2] A. K. Sharma, P. Bhardwaj, S. K. Dhawan, and Y. Sharma, Adv. Mater. Lett. **6**, 414-420 (2015).
- [3] I. Tiwari, K. P. Singh, and M. Singh, Russian Journal of General Chemistry **79**, 2685–2694 (2009)
- [4] B. Samiey, C. H. Cheng, and J. Wu, Materials **7**, 673-726 (2014); doi:10.3390/ma7020673.
- [5] <http://www.xpovder.com/>
- [6] Y. E. Shen, J. Tang, Z. H. Nie, Y. D. Wang, Y. Ren, and L. Zuo, Separation and Purification Technology **68**, 312-319 (2009).